In: Mussels: Ecology, Life Habits and Control
Editors: Jarek Nowak and Michal Kozlowski
ISBN: 978-1-62618-083-3

Chapter 4

BIOENERGETIC MODEL PREDICTIONS OF ACTUAL GROWTH AND ALLOMETRIC TRANSITIONS DURING ONTOGENY OF JUVENILE BLUE MUSSELS *MYTILUS EDULIS*

Poul S. Larsen[1], Kim Lundgreen[2] and Hans Ulrik Riisgård[2*]
[1]DTU Mechanical Engineering, Fluid Mechanics, Technical University of Denmark, Kgs. Lyngby, Denmark
[2]Marine Biological Research Centre (University of Southern Denmark), Kerteminde, Denmark

ABSTRACT

The growth rates of blue mussels *Mytilus edulis* on ropes in the Great Belt (Denmark) have been studied during the growth season of one year, from settling to about 30 mm shell length mussels, covering > 4 decades of body mass. Measured shell length (L, mm) and dry weight of soft parts (W, μg) for $L > 10$ mm followed a power-law ($W = 2.15L^{3.40}$) which supplemented an existing power-law for $L < 10$ mm ($W = 24.7\ L^{2.42}$) to establish that somatic growth changes character at $L \approx 10$ mm and $W \approx 10$ mg. Results of specific growth rates based on dry weight of soft parts ($\mu = d\ln W/dt$) compared well with predictions based on a previously developed bioenergetic growth model (BEG) for $W > 10$ mg ($\mu = aW^b$, $a = 0.871 \times C - 0.986$; $b = -0.34$, with μ in % d^{-1} and W in g) which explicitly takes into account the prevailing chl *a* concentration C (μg L^{-1}). Results for $W < 10$ mg also correlated well by the power-law ($\mu = aW^b$), now with exponent b = −0.13 close to the suggested value ($b \approx -0.1$) from experimentally established correlations for filtration and respiration rate of post-metamorphic mussels. Using the stated $W(L)$-relation for $L > 10$ mm the growth model has been expressed in terms of shell length specific growth rate ($\mu_L \equiv d\ln L/dt = \alpha L^{\beta}$) by which data on shell length was well correlated, including the influence of chl *a* concentration. Supplementary growth data from mussels in suspended net-bags at the same site illustrated differences ascribed to lack of competition for space and food, and literature data on shell length from cage-

[1] E-mail: psl@mek.dtu.dk.
[*] Corresponding author, E-mail: hur@biology.sdu.dk.

growth of mussels in the brackish Baltic Sea support the present correlations. It is argued that the allometric transitions that take place around $W \approx 10$ mg and $L \approx 10$ mm during the ontogeny of *M. edulis* is most likely universal and not restricted to first year growth of juvenile (young) mussels during the productive season.

Keywords: Energy budget, specific growth rate, ontogeny, *Mytilus edulis*, allometric transitions

INTRODUCTION

The common blue mussel, *Mytilus edulis* L. may reproduce at any time of the year, but in the temperate zone spawning is most frequent during spring and summer (Seed 1976; Dare 1976). Temperature seems to be the most important factor that determines the annual reproductive cycle, and a cold winter tends to synchronize spawning the following spring (Savage 1956; Jørgensen 1981). The fertilized egg develops to a trochophora larva that soon after becomes a free swimming veliger larva feeding on small 2 to 4 μm particles (Bayne 1965; Riisgård et al. 1980; Jespersen and Olsen 1982; Sprung 1984; Gosling 2003). This stage lasts between 3 and 5 weeks (Thorson 1961), i.e. time to reach ~300 μm, depending on environmental factors (temperature, food ration, salinity) until metamorphosis when an extensible foot appears and the larva becomes a pediveliger that settles to seek out a suitable substrate. After attachment, morphological change (metamorphosis) results in a young post-metamorphic mussel (Bayne 1965; Dare 1976; Gosling 2003; Dolmer and Stenalt 2010). The subsequent growth has been extensively investigated in both field studies, as a prerequisite to assessment of the growth potential and its exploitation in nature, and in laboratory studies (Jørgensen 1976, 1990; Stirling and Okumus 1994; Okumus and Stirling 1994; Clausen and Riisgård 1996). Many studies of growth in nature have been based on measurements of increases in shell length (e.g. Theisen 1975; Kautsky 1982; Kristensen and Lassen 1997; Dolmer 1998; Westerbom et al. 2002; Vuorinen et al. 2002) and it is therefore of interest to know the relations between growth in shell length and weight of soft parts. The present study aims at showing how bioenergetic model considerations may guide the data analysis of young post-metamorphic and juvenile/adult *M. edulis* during the productive period of a year.

The growth of filter-feeding mussels is primarily dependent on the amount of food ingested, which is closely related to the filtration rate, and the energy used in metabolism, frequently measured as the oxygen uptake rate or respiration rate. The filtration rate (F, L h^{-1}) of *Mytilus edulis* can be estimated from the dry weight of soft parts (W, g) according to the formula (Møhlenberg and Riisgård 1979): $F = a_1 W^{b1}$, where $a_1 = 7.45$ and $b_1 = 0.66$, and further, the respiration rate (R, μL O_2 h^{-1}) can be estimated according to the formula (Hamburger et al. 1983): $R = a_2 W^{b2}$, where $a_2 = 475$ and $b_2 = 0.663$. Because $b_1 \approx b_2 = 0.66$ for mussels > 10 mg tissue dry weight, it has recently been suggested by Riisgård et al. (2012a) that the weight specific growth rate may be expressed as: $\mu = aW^b$, where $b = b_1 - 1 = -0.34$. This bioenergetic growth model (BEG) predicts that the specific growth rate of mussels > 10 mg is a power function with $b = -0.34$. However, for smaller post-metamorphic mussels <10 mg dry tissue weight Hamburger et al. (1983) found that the respiration rate (R, μL O_2 h^{-1}) could be expressed as: $R = 315W(g)^{0.887}$. Further, for post-metamorphic *M. edulis* (total organic dry weight, W = 70 to 10000 μg) Riisgård et al. (1980) found that the filtration

rate (F, mL h^{-1}) could be expressed as: $F = 0.025W(\mu g)^{1.03}$. Thus for young post-metamorphic mussels < 10 mg, $b_1 \approx b_2 \approx 0.9$ which implies that the BEG model predicts $b \approx -0.1$. In a recent study on juvenile *M. edulis* Riisgård et al. (2012b) found that the ingestion rate ($I = F \times C$) increased linearly up to the incipient saturation concentration (C_{sat}; see also Riisgård et al. 2011a) and remained nearly constant above C_{sat}. But the measured weight specific growth rates (μ) decreased sharply above C_{sat} from a maximal value of about 9.5 % d^{-1} to about 1.5% d^{-1}. Below C_{sat} on the other hand, measured μ-values increased linearly with increasing algal concentration in agreement with the BEG model. Thus, the response to increasing food concentration with possible regulation of net ingestion may only come into play when C_{sat} is exceeded (Riisgård et al. 2012b).

The above considerations suggest it appropriate to present field data on mussel growth as weight specific growth rate versus dry weight of soft parts and correlate results by power-laws as done by Riisgård et al. (2012a). Among other models is the frequently used SFG (scope for growth) that is based on the energy balance, where energy available for growth is calculated from the difference between assimilated energy and respiration (e.g. Bayne and Widdows 1978; Bayne and Worrall 1980; Hawkins et al. 2001). The different energetic parameters have typically been measured in the laboratory on mussels from different sites, and the physiological response (i.e. 'scope for growth') has been used as a measure of pollution stress (e.g. Widdows et al. 1995). Two other models, MTE (metabolic theory of ecology) (Brown et al. 2004; van der Meer 2006), and DEB (dynamic energy budget) (e.g. Beadman et al. 2002; van der Veer et al. 2006; Bourlès et al. 2009; Rosland et al. 2009; Duarte et al. 2010; Saraiva et al. 2011; Filgueira et al. 2011) are likewise based on the energy budget. Here, the latter is the most general model, considering the three levels of: ecosystem, population and individual where our BEG model falls at the individual level as a "physiological component model" and has a convenient form that suggests a simple way to correlate actual field data on growth, foremost because ingestion and maintenance rates depend on the approximately same powers of size. Thus, using the simplest forms (van der Meer 2006, [Eq.1] or [Eq.4], respectively, therein), the MTE or DEB model implies that ingestion and maintenance rates depend on dry weight of soft parts (W) to powers of $b_1 = 3/4$ and $b_2 = 1$ or $b_1 = 2/3$ and $b_2 = 1$, respectively, which leads to the forms $\mu = c_1 W^{-1/4} - c_2$ or $\mu = c_3 W^{-1/3} - c_4$, respectively, where coefficients c_i depend on environmental parameters. Each of the stated forms implies growth to a finite maximal size but neither form is convenient to correlate experimental data during the productive growth period which excludes the terminal stage approaching maximal size. Also, the exponent of $b_1 = 3/4$ for ingestion is not universally valid for the whole ontogeny but has been found to be $b_1 = 0.66$ and $b_1 \approx 1$, respectively for larger and smaller blue mussels (Riisgård et al. 1980; Hamburger et al. 1983; Riisgård 1998). It should also be noted that the prediction of growth in time, given environmental parameters as pursued in MTE- and DEB-models, is a far more challenging task than the prediction of rate of growth of a given size class as pursued in the BEG-model. The present study of juvenile mussels examines the maximum individual growth rate of mussels on suspended ropes in the Great Belt (Denmark) from the early juvenile stage to young adult, and the field data are compared to bioenergetic model predictions. Additional data on mussels growing in suspended net-bags at the same site serve as reference for the growth potential when possible intra-specific competition for space and/or food on mussel-ropes is eliminated.

MATERIALS AND METHODS

Mussel-Ropes

Mussel-rope bands (5 m long by 5 cm wide, hereafter 'mussel-ropes') were set out in May 2011 at the MarBioShell research and demonstration mussel farm in Kerteminde Bay, Denmark (Figure 1), and subsequently collected at different intervals between 14 June and 9 December 2011. The densest part of the top end (1.5 m) of the farm-rope was located and a suitable piece of the mussel-rope was cut off for determination of shell length of settled mussels. Mussels on the rope were scraped off and counted along with the individuals still attached to the farm-rope by using a stereo microscope. Subsequently, shell length was determined for 3 groups; 1: a random sample of all mussels, 2: a sample of the 20 % biggest mussels, and 3: a sample of the subjectively selected 10 biggest individuals on each mussel-rope. For the samples collected later in the growth season (when mussels were >10 mm) dry weight of soft parts was also determined for Group 3 by drying the soft parts on pieces of tin foil in an oven for 24 h at 90 °C.

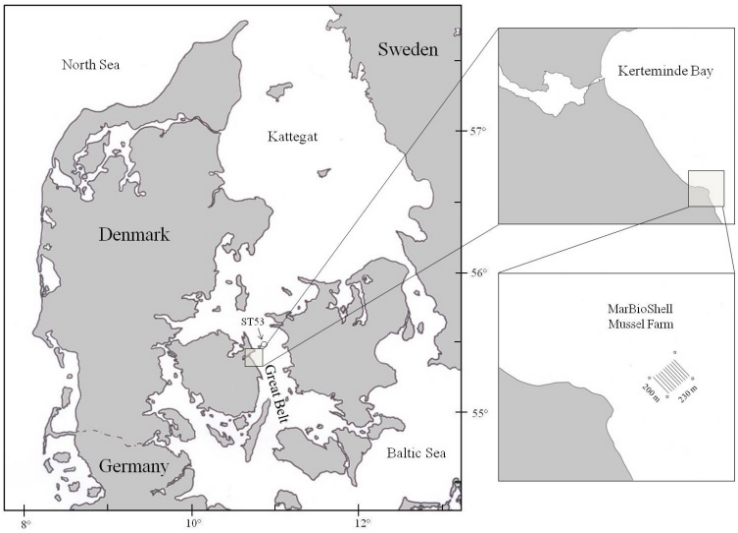

Figure 1. Map of Denmark showing the location of the MarBioShell research and demonstration mussel-farm with 10 lines for mussel production in the Great Belt (Kerteminde Bay). Farm-ropes, Series#1b and Series#2 net bags were placed on the most eastern line of the mussel farm whereas Series#1a net-bags were placed in the middle of the farm. Temperature, salinity and chl *a* were measured at ST53.

Net Bags

Mussels were collected from the MarBioShell mussel farm in September 2011 and transported to the nearby Marine Biological Research Centre (SDU) in Kerteminde and kept in large aquaria with running seawater prior to preparation for two series of field experiments with mussels hung up in net-bags.

Series #1. Mussels were divided into two size groups (mean shell length ±S.D.; 25.8±0.7 mm, n = 12 and 31.8±0.4 mm, n = 17) and put into net bags (Go Deep International Inc.). The net bags with mussels were transported to the field location site and hung up in a buoy system at the outer edge of the mussel farm 3 days before the experimental period started to allow the mussels to attach to the net material and acclimatize. At the start of the experimental period (4 October 2011; Day 0) some mussels of each of the two size groups were collected for analysis and some were transferred to the middle of the mussel farm (Figure 1). Subsequently, mussels of each size group at each location (#1a: middle and #1b: outer edge of the farm) were collected for analysis on Day 7 and Day 16. A record of chlorophyll *a* concentration, temperature and salinity near the mussel farm during the year 2011 were obtained from the Danish Nature Agency, Ministry of the Environment (Figure 2).

Series #2. Mussels were divided into two size groups (mean ±S.D.; 26.6±1.2 mm, n= 12 and 32.7±0.5, n = 17) and put into net bags (Go Deep International Inc.). The net bags with mussels were transported to the field location site and hung up in a buoy system at the outer edge of the mussel farm (Figure 1) 2 days before the experimental period started to allow the mussels to attach to the net material and acclimatize. At the start of the experimental period (10 November 2011; Day 0) mussels of each size group were collected. Subsequently, mussels of each size group were collected on Day 8 and Day 13. For both Series #1 and Series #2, collected mussels from net bags were analyzed for shell length and dry weight of soft parts.

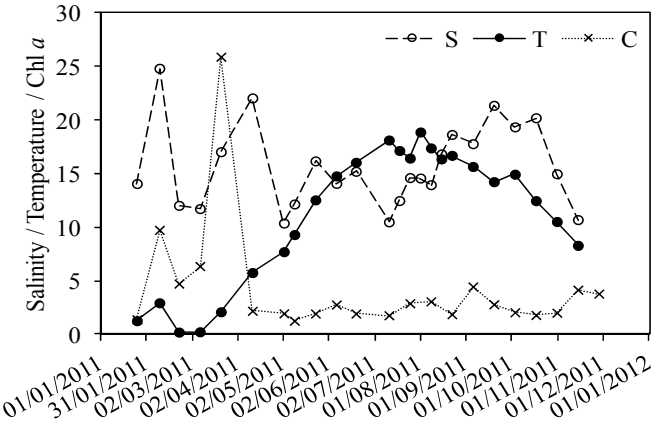

Figure 2. Environmental parameters in Great Belt during 2011. Mean (±S.D.) values were: 15.6±3.9, 11.2±6.2 and 4.1±5.2 for salinity (S, psu), temperature (T, °C) and chl *a* (C, µg L^{-1}). The high peak in chl *a* (25.9 µg L^{-1}) in March was caused by a bloom of *Chatonella* **(**Pseudochattonella farcimen). Mean (±S.D.) chl a concentration during 2011 after the bloom was 3.1±2.1 µg L^{-1}.Data obtained from Danish Nature Agency.

Equations

The dry weight of soft parts (W, µg) of young post-metamorphic *Mytilus edulis* (shell length < 10 mm) was calculated using (Jespersen and Olsen 1982):

$$W = 24.7L^{2.42}, \quad (1)$$

where L is shell length in mm. The condition index (CI, mg cm^{-3}) is given by

$$CI = W/L^3 , \tag{2}$$

where the dry weight of larger mussels was determined directly (90 °C, 24 h). Weight specific growth rates of mussels (μ, % d^{-1}) was calculated from

$$\mu = \ln(W_t/W_0)/\Delta t , \tag{3}$$

(or equivalently from the slope of the trend line in a plot of ln$W$ versus time) where W_t and W_0 are dry weight of soft parts at the end and start of growth period, respectively, and Δt is length of period in days. The average value of μ obtained this way is taken to be valid at the average dry weight of soft parts defined by

$$W_{avg} = (W_0 \times W_t)^{1/2} . \tag{4}$$

The estimated weight specific growth rate (μ_{est}, % d^{-1}) for mussels > 10 mg according to the BEG model (Riisgård et al. 2012a, Eq.18 therein) is

$$\mu_{est} = aW^b, \ (a = 0.871 \times C - 0.986; \ b = -0.34) , \tag{5}$$

where W (g) is dry weight of soft tissue and C (µg L^{-1}) the chlorophyll a concentration. Using the definition, $\mu = (1/W)\mathrm{d}W/\mathrm{d}t$, and the power-law of Eq.(5), i.e. $\mu \equiv (1/W)\mathrm{d}W/\mathrm{d}t = aW^b$, or $W^{-(1+b)}\mathrm{d}W = -(1/b)\mathrm{d}W^{-b} = a\mathrm{d}t$, the time history of growth from a given initial size (W_1 at time t_1) is obtained by integration, yielding $W^{-b} - W_1^{-b} = -ba(t - t_1)$, or

$$W = [W_1^{-b} + (-ba)(t - t_1)]^{-1/b} . \tag{6}$$

In the same way, defining the shell length specific growth rate (μ_L, d^{-1}) by

$$\mu_L \equiv (1/L)\mathrm{d}L/\mathrm{d}t = \mathrm{d}\ln L/\mathrm{d}t \approx \ln(L_t/L_0)/\Delta t , \tag{7}$$

where L_t and L_0 are shell length at the end and start of growth period, respectively, and Δt is length of period in days, and assuming the validity of a power-law for shell growth over some size range,

$$\mu_L = \alpha L^{\beta} . \tag{8}$$

The time history of shell growth from a given initial size (L_1 at time t_1) is obtained by integration (as for Eq.6), yielding

$$L = [L_1^{-\beta} + (-\beta\alpha)(t - t_1)]^{-1/\beta} . \tag{9}$$

Values of μ_L may be calculated from shell length data $L(t)$ in the same way as μ from $W(t)$ in Eq.(3), or equivalently from the slope of the trend line in a plot of ln$L$ versus time.

Average values of μ_L obtained this way over a time interval from 0 to t is taken to be valid at the average shell length defined by

$$L_{avg} = (L_0 \times L_t)^{1/2} . \quad (10)$$

We may also relate μ_L to μ by introducing the power-law $W = cL^d$ into Eq.(5) which gives $\mu = d\ln W/dt = d\ d\ln L/dt = d\ \mu_L$, hence

$$\mu_L = \mu/d = (a/d)W^b , \quad (11)$$

from which W is finally eliminated by using again $W = cL^d$, leaving

$$\mu_{L,est} = \alpha L^\beta ; \alpha = a/(dc^b) , \beta = bd . \quad (12)$$

Statistics

Pearson Product Moment Correlation (PPMC) was carried out in SigmaPlot and used to measure the strength of the correlation between dry weight of soft parts and weight specific growth rate, and shell length and shell length specific growth rate. The hypothesis that slopes were significantly different from zero was accepted for $P < 0.05$. Analysis of Covariance (ANCOVA) was carried out in Systat and used for investigation if slopes of correlations between dry weight of soft parts and weight specific growth rate, and shell length and shell length specific growth rate were different between groups of mussels. Hypothesis of significant difference of slopes was accepted for $P > 0.05$.

RESULTS

Veliger Larvae and Settling

The time domain of the study covered most of the year 2011. Figure 3 shows the occurrence of veliger larvae in the vicinity of the suspended mussel-ropes, averaging 2 ind. L^{-1} during May to June, and 1 ind. L^{-1} during July to August whereupon the density fades out. At the start of farm-rope data collection on 14 June, settled larvae had an average length of 0.6 mm (Table 1, Group 1). The density of settled individuals then quickly increased to peak late in July after which the density declined, but the recorded mean shell lengths of all of the 3 groups continued to increase (Figure 4, Table 1).

Mussel-Ropes

Growth versus time in terms of shell length (L) is summarized in Table 1 and Figure 4 for the 3 selected groups of mussels: Group 1 (s) random samples of all sizes, Group 2 (20 %) the 20 % biggest individuals, and Group 3 (10) the 10 biggest individuals. Growth versus time in

terms of dry weight of soft parts (W) is summarized in Table 2 for Group 3 of 10 biggest mussels, both as estimated from shell length according to Eq.(1) and, for $W > 10$ mg as measured directly. Using these results and Eq.(3) give the tabulated values of weight specific growth rates (μ) versus average dry weight (W_{avg}, Eq.4), also shown in the log-log plot of Figure 5. To show the change in weight specific growth rates versus time we have plotted ln$W$ versus time in Figure 6 where the slope of lines through successive points, according to Eq.(3), gives the same average value μ over time intervals as listed in Table 2. Further, the exponent of a regression line through the first 3 of the 4 data points from measured dry weight of soft parts (W_0 of Table 2) versus time, Figure 7, gives the average specific growth rate ($\mu = 5.37$ % d^{-1}) during the period from 27 July to 4 October.

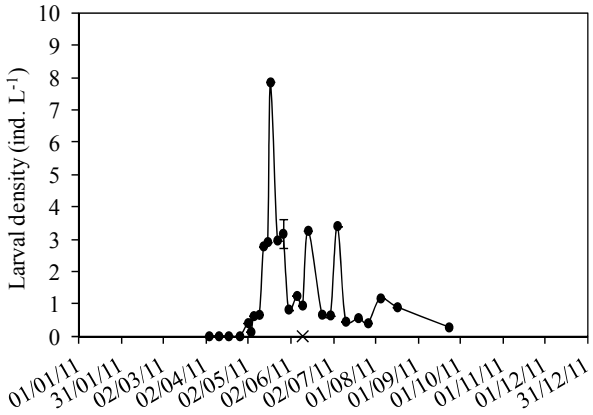

Figure 3. *Mytilus edulis*. Density of mussel veliger larvae at the experimental site. The cross marks the date (10 June 2011) when the first settling of pediveliger larvae on farm-ropes was observed.

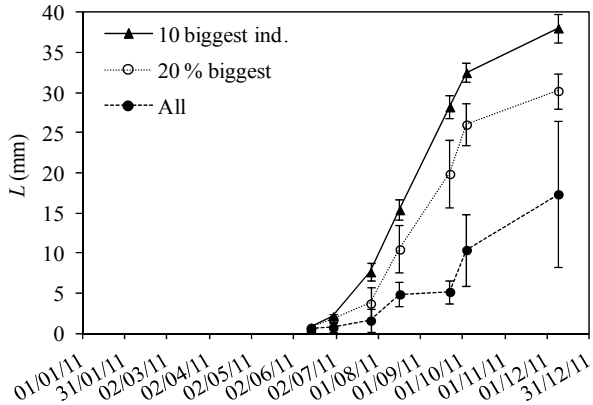

Figure 4. *Mytilus edulis* (farm-ropes, Groups 1, 2 and 3). Mean (±S.D.) shell length (L, mm) mussels for each of 3 groups: (1) all mussels on farm-ropes, (2) biggest 20%, and (3) 10 biggest individuals found on the rope.

Table 1. *Mytilus edulis* (farm-ropes).
Growth parameters for mussels in the period
14 June to 9 December 2011

		Rope-segment			Group 1			Group 2					Group 3			
Date 2011	Δt (d)	n_{tot}	RS (cm)	D (ind. cm^{-1})	n_s	L (mm)	ΔL (mm mo^{-1})	$n_{20\%}$	L (mm)	ΔL (mm mo^{-1})	L_{avg} (mm)	μ_L (d^{-1})	L (mm)	ΔL (mm mo^{-1})	L_{avg} (mm)	μ_L (d^{-1})
14-06	0	48	5	10	48	0.6±0.1		10	0.8±0.1				0.8±0.1			
30-06	16	292	5	58	146	0.8±0.6	0.5	29	1.8±0.3	2.0	1.17	0.0848	2.2±0.3	2.7	1.28	0.0632
27-07	27	1454	5	291	522	1.7±1.5	1.0	104	3.8±2.1	2.2	3.84	0.0379	7.7±1.1	6.2	4.10	0.0464
17-08	21	864	5	173	145	4.9±1.5	4.7	29	10.5±3.0	9.8	9.53	0.0379	15.4±1.3	11.2	10.90	0.0330
22-09	36	4453	21	212	255	5.2±1.4	0.3	51	19.9±4.2	7.9	19.18	0.0167	28.3±1.4	10.8	20.88	0.0169
11-10	12	3741	44	85	136	10.5±4.4	13.2	27	26.1±2.6	15.6	27.50	0.0100	32.5±1.2	10.8	30.31	0.0115
09-12	66	1855	35	53	91	17.4±9.1	3.2	18	30.3±2.2	1.9	30.23	0.0011	38.1±1.8	2.6	35.19	0.0024

Δt = days since last subsample; n_{tot} = total number of mussels on farm-rope segment sample; n_s = number of randomly collected mussels in sample for shell length measurement (Group 1); $n_{20\%}$ = number of mussels from the 20 % biggest individuals of the sample n_s (Group 2); 10 biggest mussels found on farm-rope (Group 3); RS = rope segment; D = density; L = shell length of mussels in group; ΔL = increase in shell length since last subsample; L_{avg} = average shell length, Eq.(10); μ_L = shell length specific growth rate, Eq.(7). Mean±S.D. are shown.

Table 2. *Mytilus edulis* (farm-ropes, Group 3: 10 biggest individuals)

				Calculated Eq. (1)				Measured			
Growth period 2011	Δt (d)	T (°C)	C (µg L^{-1})	W_0 (mg)	W_{end} (mg)	W_{avg} (mg)	μ_{cal} (% d^{-1})	W_0 (mg)	W_{end} (mg)	W_{avg} (mg)	μ (% d^{-1})
14 Jun – 30 Jun	16	16.0	1.9	0.013	0.163	0.05	16.0				
30 Jun – 27 Jul	27	17.2±0.8	2.3±0.8	0.163	3.45	0.75	11.3				
27 Jul – 17 Aug	21	17.5±1.3	3.1	3.45	18.6	8.0	8.0	3.45*	23.5	9.0	9.1
17 Aug – 22 Sep	36	15.5±1.2	3.0±1.3	18.6	80.2	38.6	4.1	23.5	182.3	65.5	5.7
22 Sep – 04 Oct	12	14.9	2.0	80.2	112.7	95.1	2.8	182.3	296.0	232.3	4.0
04 Oct – 09 Dec	66	11.5±2.8	2.9±1.2	112.7	165.3	136.5	0.6	296.0	242.3	267.8	-0.3

Growth periods, lengths of growth periods (Δt), mean temperature in period (T), mean chl *a* (C), dry weight of soft parts at start (W_0) and end (W_{end}) of growth periods, average dry weight of soft parts in growth period (W_{avg}, Eq.4) and corresponding weight specific growth rates (μ, Eq.3) are presented as calculated from shell length data using Eq. (1), and as actually measured body dry weight on collected mussels with shell length >10 mm. Mean±S.D. are shown.*Calculated.

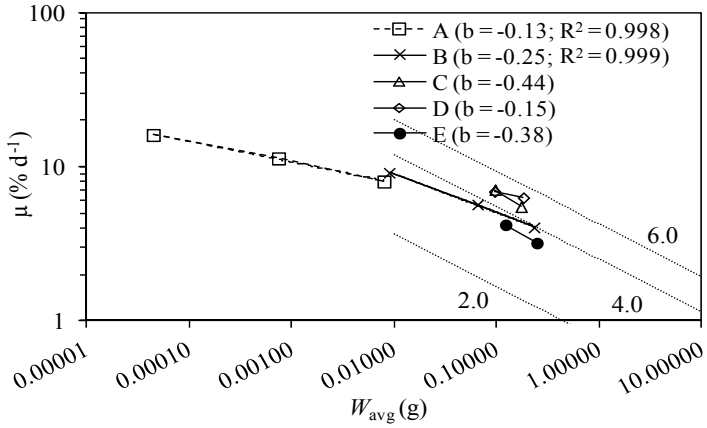

Figure 5. *Mytilus edulis*. Weight specific growth rate (μ, from Tables 2 and 3) versus average body dry weight (Eq.4). Power-law exponent of regression lines (*b*) are shown in the figure. A: small farm-rope mussels (W_{avg} < 10 mg), B: larger farm-rope mussels (W_{avg} > 10 mg), C and D: net-bag mussels, Series #1a, 1#b in October 2011, and E: Series #2 in November 2011. Dotted lines: growth model (Eq.5) for 3 values of chl *a* concentration (μg L^{-1}).

As a supplement to the allometry of Eq.(1) valid for young post-metamorphic *Mytilus edulis* (shell length < 10 mm) a plot (Figure 8) of the measured values of both dry weight of soft parts (*W*, μg) and shell length (*L*, mm) of larger mussels (> 10 mm) during growth (from 17 August to 4 October) shows good agreement with the power law: $W = 2.15L^{3.40}$. To show growth of shell length in terms of shell length specific growth rate (Eq.7) we have plotted ln*L* versus time (not shown but similar to Figure 6 for *W*) in which the slope of lines through successive points gives the average value μ_L over time intervals as listed in Table 1 for Groups 2 and 3. These results versus average length (L_{avg}, Eq.10) are shown in the log-log plot of Figure 9 in which coefficients (α and β of Eq.12) of regression lines are given.

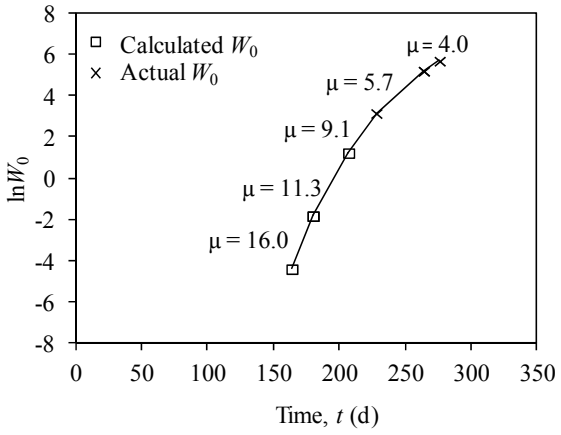

Figure 6. *Mytilus edulis* (farm-ropes, Group 3). Semi-logarithmic plot of dry weight of soft parts (W_0, mg; Table 2), either calculated from measured shell length (Eq.1) of small post-metamorphic mussels (□) or from actual measurement of soft parts (x), versus time. The weight specific growth rates (μ, % d^{-1}) calculated by means of Eq.(3) for all growth periods are indicated.

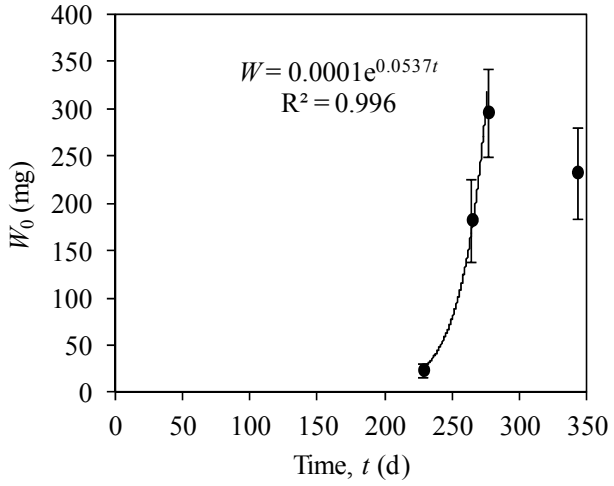

Figure 7. *Mytilus edulis* (farm-ropes, Group 3). Measured dry weight of soft parts (W_0, Table 2) of the 4 last samples versus time (Day 0 = 1 January 2011. The exponent of the exponential trend line, excluding the last sample, shows a mean weight specific growth rate (μ) of 5.37 % d^{-1}.

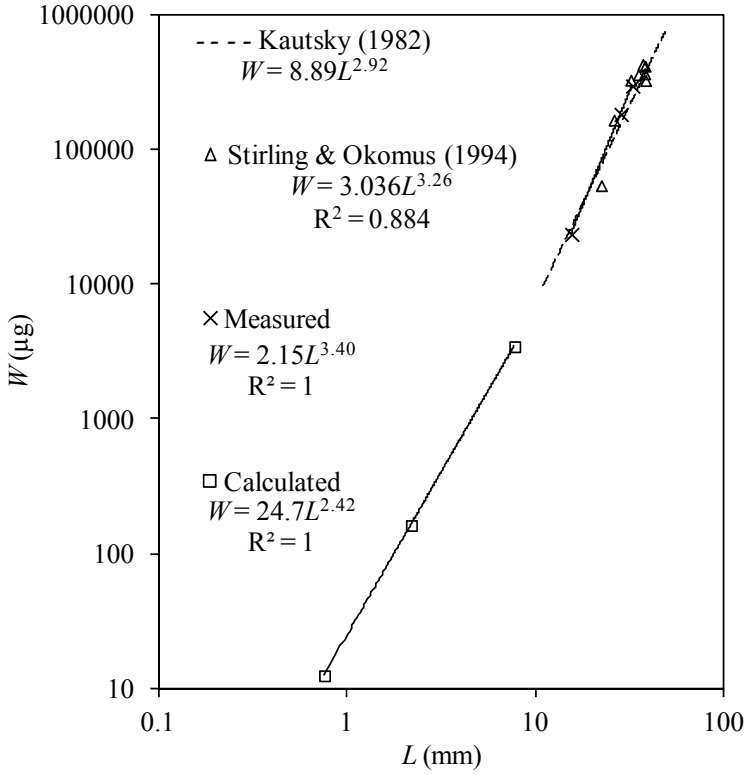

Figure 8. *Mytilus edulis* (farm-ropes, Group 3). Dry weight of soft parts calculated (Eq.1) for young post-metamorphic mussels (□) and measured (Eq.13) for larger juvenile mussels (×), both versus measured shell length (Table 2). Correlation of Kautsky (1982, Figure 17 therein) (dotted line). $W(L)$ from Stirling and Okumus (1994, their Series LL) includes data from May to November 1991 (Δ), after which chl *a* concentration falls below 0.2 μg L^{-1} and dry weight started to decrease.

Net-Bags

Growth in terms of shell length (*L*), measured dry weight of soft parts (*W*), calculated specific growth rate (μ) and condition index (*CI*) for the 2 size groups of mussels at each of Series #1a, #1b and Series #2 are summarized in Table 3 and Figures 10 and 11. The determined values of μ and μ_L from these series have also been shown in Figure 5 and Figure 9, respectively, for comparison with results from mussel-ropes.

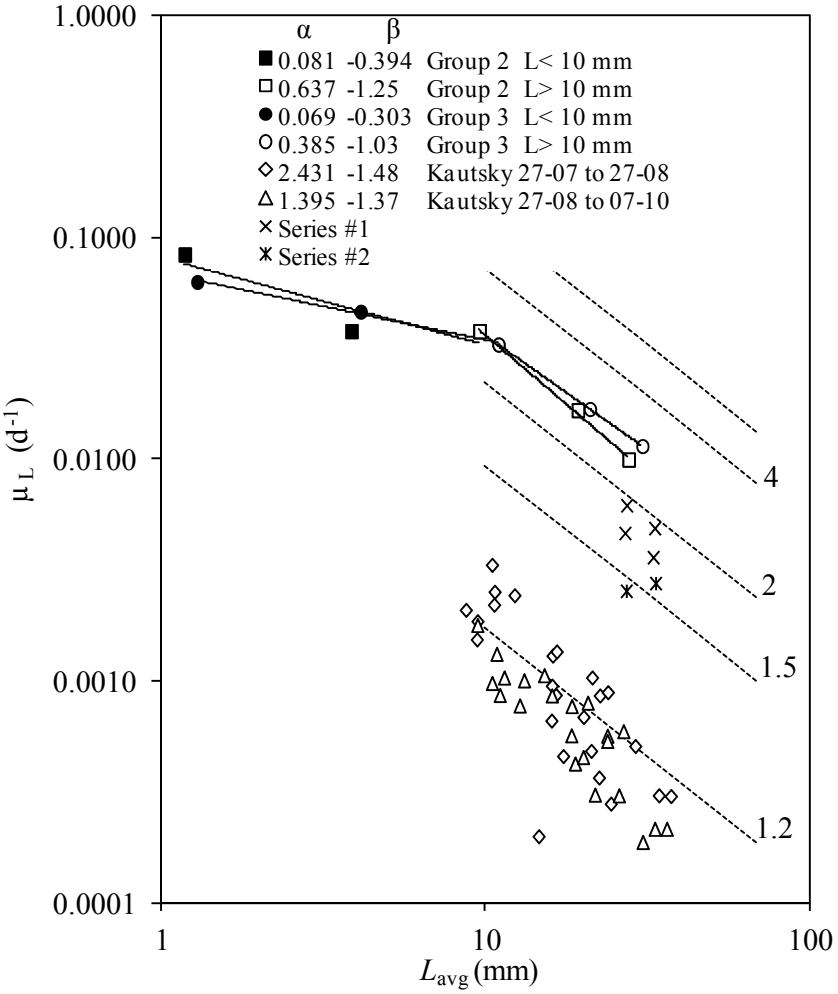

Figure 9. *Mytilus edulis* (farm-ropes: Groups 2 and 3; net-bags: Series #1 and #2). Shell length specific growth rate (μ_L, Eq.7) versus average shell length (L_{avg}, Eq.10) over each successive growth interval, cf. Table 1. Coefficients of power-law relations for present data of shell length smaller and larger than about 10 mm, as well as for re-plotted data for $L_{avg} > 10$ mm from Kautsky (1982, Figure 5 therein) are inserted in figure. Dotted lines: growth model (Eq.12) for 5 values of chl *a* concentration (μg L^{-1}).

Table 3. *Mytilus edulis* (net-bags, Series #1a, #1b and Series #2)

Series # Date 2011	Δt (d)	Chl *a* ($\mu g\ L^{-1}$)	*T* (°C)	*S* (psu)	L_0 (mm)	L_{end} (mm)	L_{avg} (mm)	μ_L (d^{-1})	W_0 (mg)	W_{end} (mg)	W_{avg} (mg)	μ (% d^{-1})	CI_0 (mg cm^{-3})	CI_{end} (mg cm^{-3})
#1a	16	1.9±0.2	13.7±1.7	19.8	25.8±0.7	28.5±0.9	27.1	0.00622	55.3±12.7	171.9±47.3	97.5	7.1	3.2±0.7	7.3±1.6
4−20 Oct					31.8±0.4	33.7±1.1	32.7	0.00363	111.8±20.8	269.2±45.1	173.5	5.5	3.5±0.7	7.0±0.8
#1b	16	1.9±0.2	13.7±1.7	19.8	25.8±0.7	27.8±1.3	26.8	0.00467	55.3±12.7	167.6±53.8	96.3	6.9	3.2±0.7	7.6±2.0
4−20 Oct					31.8±0.4	34.4±0.8	33.1	0.00491	111.8±20.8	301.0±46.0	183.5	6.3	3.5±0.7	7.4±1.0
#2	13	3.3±1.1	9.4±1.6	12.8	26.6±1.2	27.5±0.8	27.0	0.00256	92.2±17.0	163.3±22.3	122.7	4.2	4.9±0.6	7.9±0.8
10−23 Nov					32.7±0.5	33.9±0.5	33.3	0.00277	199.6±41.4	309.1±49.7	248.4	3.2	5.7±1.2	8.0±1.2

Duration (Δt) of mussel growth in net-bags at MarBioShell mussel farm, mean (±S.D.) values of chlorophyll *a* (chl *a*), temperature (*T*), salinity (*S*), initial shell length (L_0), body dry weight (W_0), initial condition index (CI_0, Eq.2), final shell length (L_{end}), final body dry weight ($W_{end,}$), final condition index (CI_{end}), average shell length and body dry weight (L_{avg} and W_{avg} from Eq.10 and 4), and average shell length and weight specific growth rates (μ_L from table values and μ from slopes in Figures 10a and 10b). n = 10-17. Chl *a*, temperature and salinity data are obtained from the Danish Nature Agency.

DISCUSSION

Mussel-Ropes

For Group 3 of 10 biggest mussels on farm-ropes, results of the specific growth rate during the growth season in Figure 5 are seen to follow the power-law ($\mu = aW^b$) quite well in the two size ranges: for small farm-rope mussels ($W_{avg} < 10$ mg) with exponent $b = -0.13$, which is close to the suggested value of $b = -0.1$, and for larger farm-rope mussels ($W_{avg} > 10$ mg) with exponent $b = -0.25$, which is somewhat larger than $b = -0.34$ predicted by the BEG model. However, it is noted that the dotted lines of the growth model in Figure 5 indicate a predicted ambient chl *a* concentration of about 3 to 4 μg L^{-1} in fair agreement with the general level of observed average chl *a* concentration (3.1±2.1 μg L^{-1}, Figure 2) at the site during the period. Statistical treatment (PPMC) reveals that slopes describing the correlation between dry weight of soft parts and weight specific growth rate are significantly different from zero (Group 1: $r_p = -0.999$, N = 3, P = 0.0284; Group 2: $r_p = -0.999$, N = 3, P = 0.0216), and the slopes are significantly different between mussel groups (ANCOVA, $F_{(1,3)} = 0.243$, P = 0.656).

It is interesting to note that the correlation of data from a growth experiment with *Mytilus edulis* of $L > 10$ mm kept one year in cages could be expressed as: $W(\mu g) = 8.90L(mm)^{2.92}$ by Kautsky (1982, Figure 17 therein) which is near identical to that of Eq.(13) as shown in Figure 8. The same is true for data of Stirling and Okumuş (1994, re-plotted from their Figures 3 and 4) on year old rope-grown blue mussels > 10 mm on the west coast of Scotland at Loch Etive (LE) and Loch Leven (LL) during May-Sept (having regression lines of $W = 61.24L^{2.45}$ and $W = 3.04L^{3.26}$, respectively). Later in the season, however, data fall below these regression lines as the chl *a* concentration decreases to values well below 0.6 μg L^{-1}. (To convert the "ash-free dry meat weight" given by Stirling and Okumuş (1994) into dry weight of soft parts we have multiplied by a factor 1.1; own determination of conversion factor). Our previous results (Riisgård et al. 2011b, Figure 12 therein) on mussels ($16<L<83$ mm) collected in Kerteminde Fjord, Denmark, were correlated by $W = 6.0L^{3.0}$ which is close to the foregoing correlations, confirming the general trend of dry weight of soft parts being approximately proportional to L^3 for $L > 10$ mm. Further, equating Eqs.(1) and (13) shows that the 2 regression lines in Figure 8 intersect at $L = 12.1$ mm, corresponding to $W = 10.3$ mg in good agreement with the change-over observed in Figure 5. These results confirm that increase of body dry weight and shell length during the ontogeny of *M. edulis* changes character around $W \approx 10$ mg and $L \approx 10$ mm. However, these allometric transitions are probably smooth and they remain to be explained biologically.

The weight specific growth rate μ is a useful quantity because it does not explicitly involve absolute time but only time intervals to give the instantaneous rate of growth for a given size W of mussel. Knowing $\mu(W)$, however, the time history of growth from a given initial size (W_1 at time t_1) can be obtained by integration, which becomes simple (Eq.6) when $\mu(W)$ follows a power law as suggested by the BEG model. The same is true for growth in terms of shell length where the data supported correlation of form $W = cL^d$ (Figure 8) for small and large mussels transforms the power law of the BEG model ($\mu = aW^b$) into a power law for shell length specific growth rate (μ_L, Eq.12). The present μ_L-values for Groups 2 and 3 (Table 1) are plotted versus L_{avg} in Figure 9. Inspection indicates that both groups follow

power-law trends with exponents $\beta = -0.394$ and -0.303, respectively, for shell length < 10 mm, and exponents $\beta = -1.25$ and -1.03, respectively, for shell length > 10 mm, the correlation coefficients of the two data sets being 0.99 and 1.00, respectively. This means that the growth of the 10 biggest mussels is quite representative of the biggest 20% of all of the population, and we used the averages of exponents $\beta = -0.352$ and 1.12, respectively, and the averages of coefficient $\alpha = 0.0755$ and 0.480, respectively (obtained from regression to the 2 groups of data jointly) to predict growth by Eq.(9) for $L < 10$ and > 10 mm, respectively, in preparing Figure 9. Statistical treatment (PPMC) reveals that slopes describing the correlation between shell length and shell length specific growth rate are significantly different from zero for both groups of mussels < 10 mm ($r_p = -0.861$, N = 6, P = 0.028) and > 10 mm ($r_p = -0.901$, N = 6, P = 0.014) shell length. Slopes of regression lines between groups are significantly different from each other (ANCOVA, $F_{(1,9)} = 0.623$, P = 0.450).

In general, μ_L of Eq.(8) may prove to be a useful relation for studies of mussel growth if only measured in terms of shell length. It was used by Kautsky (1982, his Figure 5 and Table 1, in a form based on $\log_{10}L$ in place of $\ln L$) to study cage-growth of mussels in the brackish Baltic Sea near the Askö Laboratory during different seasons. Some of these results for $L >$ 10 mm (appropriately converted into the present μ_L-values) have been re-plotted in Figure 9 and appear to be correlated by Eq.(8) with β-values close to those of the present data, but the magnitude of growth (α-value) is 10 to 20 times lower than found for mussels on farm-ropes in the Great Belt in the present study. The slow growth may however be explained by a low salinity of around 7 psu at the growth site on the Swedish Baltic coast and a low mean annual chlorophyll *a* concentration of approximately 1.5 μg L^{-1} (Kautsky 2008). More specifically according to Ulf Larsson (personal communication), the mean annual chl *a* for the Askö waters was 1.56 μg L^{-1} for the 34 year period from 1976 to 2009 with variations from 1.11 μg L^{-1} (1989) to 2.46 μg L^{-1} (2008, sole year with chl *a* > 2 μg L^{-1}) measured on water samples collected at least 20 times per year in the upper 20 m (cf. the Swedish data base SMHI, www.smhi.se). For this reason the model predictions from Eq.(12) have also been shown in Figure 9 (dotted lines) for a number of values of chl *a* which suggest that the chl *a* concentration might have been as low as 1.2 μg L^{-1} provided feeding conditions were otherwise close to optimal and no effect of low salinity. Other data (Kautsky 1982, Figure 22 therein) confirm the slow growth, taking of the order of 10 to 12 years to reach a shell length of 30 mm as compared to about one year at the present Great Belt site. Growth rate and maximum size of *Mytilus edulis* is much lower in the brackish Baltic Sea (7 psu) than in the high saline North Sea (28 psu), but reciprocally transplanted mussels grew at rates similar to those of native mussels at each site (Kautsky et al. 1990), indicating that the observed variations in growth may be explained by differences in salinity and chl *a*. Other observations of shell growth rates from the northern Baltic Sea (4.5 psu) include Westerbom et al. (2002, Figure 6 therein): 12 years to reach 30 mm with max. 2.9 mm y^{-1}; Vuorinen et al. (2002, Figure 6 therein): 8 years to reach 30 to 35 mm. For comparison, Schütz (1964) states that mussels at the Kiel Bight (18 psu) attain a shell length of 30 mm during the first year, as also found in the present study (16 psu, Figure 2). We have also calculated $\mu_L(L_{avg})$ for data from Stirling and Okumus (1994, their Series LE and LL) and when plotted in Figure 9 (not shown) the results scatter around the present data shown from Series #1 and #2 near $C = 1.5$ to 2 μg L^{-1} according to the BEG-model in accord with the low chl *a* concentrations given by Stirling and Okumus (1994). However, it should be noted that spawning cycle and other factors may lead to changes in the relationship between shell length (L) and dry weight of soft

parts (W) (e.g. Dare 1976), hence of the condition index ($CI = W/L^3$), as seen from the variation of such values in Table 3.

Net-Bags

Series #1a and #1b. The weight specific growth rates were high both within the mussel farm, between 5.5 and 7.1 % d^{-1} for 31.8 and 25.8 mm shell length mussels, respectively (Table 3, Figure 10), and at the outer edge of the farm, 6.3 and 6.9 % d^{-1} for 31.8 and 25.8 mm mussels, respectively, compared to a previous study in the same area (Riisgård et al. 2012a). This suggests optimal conditions with no negative effects of e.g. high current speeds or changing salinities during the growth period and that the mean chl *a* concentration in the surrounding water must have been relatively high during the growth period, which according to the growth model shown in Figure 5 should have been around 5 µg L^{-1}, but the actually measured mean concentration from October 2011 was low, about 1.9±0.2 µg L^{-1} (Figure 2, Table 3). Further, Figure 5 (data C and D) shows that there is no significant difference between growth of net-bag mussels in the middle (#1a) or in the outer region (#1b) of the farm site, and the higher growth rates than those of farm-rope mussels of the same size could be a result of less intraspecific competition for nutrition (Fréchette et al. 1992).

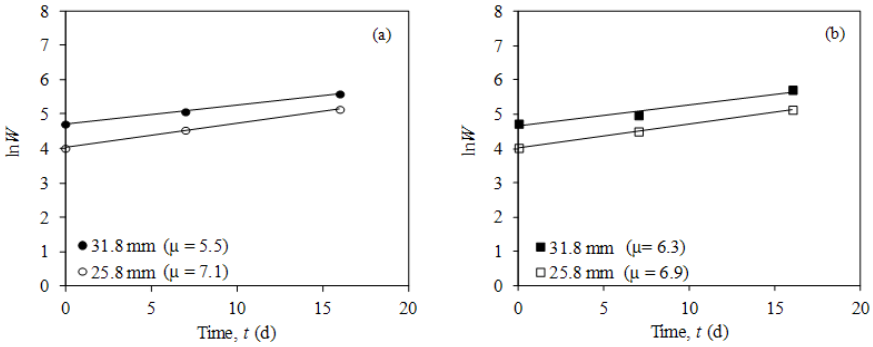

Figure 10. *Mytilus edulis* (net-bags, Series #1a, #1b). Growth data in terms of ln$W$ during the period 4 to 20 October 2011. Series #1a (a) are mussels suspended within the mussel farm, and Series #1b (b) are mussels suspended at the outer edge of the mussel-farm. µ (% d^{-1}) shows the average weight specific growth rate of the 2 size classes in the growth period.

Series #2. The weight specific growth rates were 4.2 and 3.2 % d^{-1} for 26.6 and 32.7 mm shell length mussels, respectively (Table 3, Figure 11), which according to the dotted lines of the growth model in Figure 5 indicate a predicted ambient chl *a* concentration of about 3.5 µg L^{-1} in good agreement with the actual concentration from November 2011 of 3.3±1.1 µg L^{-1} (Figure 2, Table 3). μ_L-values in Figure 9, on the other hand, suggest the much lower chl *a* value of $C \sim 1.5$ µg L^{-1}.

These inconsistencies may be a result of seasonal differences in growth between Series #1 (4 to 20 Oct) and Series #2 (10 to 23 Nov) such that Series #2 falls outside of the favorable growth period intended for study, just as the last data points of Tables 1 and 2 were ignored.

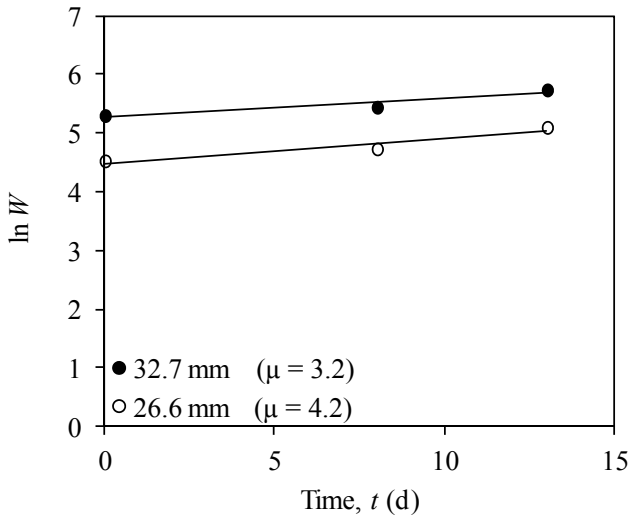

Figure 11. *Mytilus edulis* (net-bags, Series #2). Growth data in terms of ln*W* of mussels suspended at the outer edge of the mussel-farm during the period 10 to 23 November 2011. μ (% d^{-1}) shows the average weight specific growth rate of the 2 size classes in the growth period.

It is notable that the calculated values of shell length specific growth rates μ_L for Series #1 and #2 shown in Figure 9 are low compared to the shell growth of Groups 2 and 3 and that this is not the case for the weight specific growth rates μ of these groups in Figure 5. This phenomenon may probably be explained by delayed growth of shells compared to somatic growth of net-bag mussels with an initially low condition index, cf. about doubling of *CI* in the field-growth period (Table 3).

CONCLUSION

The present growth data of juvenile mussels on ropes, supplemented by growth data of mussels in suspended net-bags at the same site, support the bioenergetic growth model of Eq.(5) for $W > 10$ mg ($b = -0.34$) and the modified form for $W < 10$ mg ($b \approx -0.13$), covering more than 4 decades of size in terms of dry weight of soft parts (W) as shown in Figure 5. From the growth data on shell length (L), leading to Eq.(13) to supplement Eq.(1) and leading to Figure 9, it has been experimentally confirmed that increase of body dry weight (somatic growth) and shell length during the ontogeny of the blue mussel changes character around $W \approx 10$ mg and $L \approx 10$ mm. Further, using Eqs.(1) and (13), the somatic growth model has been expressed in terms of shell length as Eq.(12) and used to show that other field data on mussel growth in the Baltic Sea (Kautsky 1982) lends well to interpretation by the model. The explicit model dependence on chlorophyll *a* concentration is well established for larger mussels ($W > 10$ mg) for which model predictions have been compared to actual growth rates in the field, but similar predictions remains to be established for smaller mussels ($W < 10$ mg), along with other environmental parameters such as salinity and current velocity. It is well known that e.g. Dutch and English fishermen transplant small mussels stagnant in growth from the intertidal level to below the tidal level where the mussels quickly grow to marketable sizes (Baird 1966). Because the potential for growth "remains intact for many

years in mussels that have been prevented from exploiting it owing to unfavorable environmental conditions" (Jørgensen 1976) the present statement that allometric transitions take place around $W \approx 10$ mg and $L \approx 10$ mm during the ontogeny of *Mytilus edulis* is most likely universal, and not restricted to first year growth of juvenile (young) mussels during the productive season.

ACKNOWLEDGMENTS

This work formed part of the MarBioShell project supported by the Danish Agency for Science, Technology and Innovation for the period January 2008 to December 2012. Thanks are due to Dr. Daniel Pleissner for helpful assistance with statistics, to Prof. Ragnar Elmgren for valuable information, and to Lene Simonsen and Maria Ángeles Provencio López for technical assistance.

REFERENCES

Baird RH (1966) Factors affecting the growth and condition of mussels (*Mytilus edulis* L.). *Fish Invest Ser II* 25, No 2, 1−33.

Bayne BL (1965) Growth and the delay of metamorphosis of the larvae of *Mytilus edulis*. *Ophelia* 2:1-47.

Bayne BL, Widdows J (1978) The physiological ecology of two populations of *Mytilus edulis* L. *Oecologia* (Berl) 37:137−162.

Bayne BL, Worrall CM (1980) Growth and production of mussels *Mytilus edulis* from two populations. *Mar Ecol Prog Ser* 3:317−328.

Beadman HA, Willows RI, Kaiser MJ (2002) Potential applications of mussel modeling. *Helgoland Mar Res* 56:76−85.

Bourlès Y, Alunno-Bruscia M, Pouvreau S, Tollu G, Leguay D, Arnaud C (2009) Modelling growth and reproduction of the Pacific oyster *Crassostrea gigas*: Advances in the oyster-DEB model through application to a coastal pond. *J Sea Res* 62:62−71.

Brown JH, Gillooly JF, Allen AP, Savage VM, West GB (2004) Toward a metabolic theory of ecology. *Ecol* 85:1771−1789.

Clausen I, Riisgård HU (1996) Growth, filtration and respiration in the mussel *Mytilus edulis*: no regulation of the filter-pump to nutritional needs. *Mar Ecol Prog Ser* 141:37−45.

Dare PJ (1976) Settlement, growth and production of the mussel, *Mytilus edulis* L., in Morecambe Bay, England. Fish Invest Ser II 28, No 1, 1−25.

Dolmer P (1998) Seasonal and spatial variability in growth of *Mytilus edulis* L. in a brackish sound: comparisons of individual mussel growth and growth of size classes. *Fish Res* 34: 17−26.

Dolmer P, Stenalt E (2010) The impact of the adult blue mussel (*Mytilus edulis*) population on settling of conspecific larvae. *Aquacult Int* 18:3−17.

Duarte P, Fernández-Reiriz MJ, Filgueira R, Labarta U (2010) Modelling mussel growth in ecosystems with low suspended matter loads. *J Sea Res* 64:273−286.

Filgueira R, Rosland R, Grant J (2011) A comparison of scope for growth (SFG) and dynamic energy budget (DEB) models applied to the blue mussel (*Mytilus edulis*). *J Sea Res* 66:403-410.

Fréchette M, Aitken AE, Pagé L (1992) Interdependence of food and space limitation of a benthic suspension feeder: consequences for self-thinning relationships. *Mar Ecol Prog Ser* 83:55−62.

Gosling E (2003) Bivalve molluscs. Biology, ecology and culture. Fishing News Books, Blackwell, p 443.

Hamburger K, Møhlenberg F, Randløv A, Riisgård HU (1983) Size, oxygen consumption and growth in the mussel *Mytilus edulis*. *Mar Biol* 75:303−306.

Hawkins AJS, Fang JG, Pascoe PL, Zhang JH, Zhang XI, Zhu MY (2001) Modelling short-term responsive adjustments in particle clearance rate among bivalve suspension-feeders: separate unimodal models of seston volume and composition in the scallop *Chlamys farreri*. *J Exp Mar Biol Ecol* 261:61−73.

Jespersen H, Olsen K (1982) Bioenergetics in veliger larvae of *Mytilus edulis* L. *Ophelia* 21:101−113.

Jørgensen CB (1976) Growth efficiencies and factors controlling size in some mytilid bivalves, especially *Mytilus edulis* L.: review and interpretation. *Ophelia* 15:175−192.

Jørgensen CB (1981) Mortality, growth, and grazing impact of a cohort of bivalve larvae, *Mytilus edulis* L. *Ophelia* 20:185−192.

Jørgensen CB (1990) Bivalve filter feeding: hydrodynamics, bioenergetics, physiology and ecology. Olsen & Olsen, Fredensborg, Denmark. 140 pages.

Kautsky N (1982) Growth and size structure in a Baltic *Mytilus edulis* population. *Mar Biol* 68:117−133.

Kautsky H (2008) Askö area and Himmerfjärden. In: Schiewer U (ed) Ecology of Baltic coastal waters. Ecological studies 197. Springer-Verlag Berlin Heidelberg, pp 335−360.

Kautsky N, Johannesson K, Tedengren M (1990) Genotypic and phenotypic differences between Baltic and North Sea populations of *Mytilus edulis* evaluated through reciprocal transplantations. I. Growth and morphology. *Mar Ecol Prog Ser* 59:203-210.

Kristensen PS, Lassen H (1997) The production of relaid blue mussels (*Mytilus edulis* L.) in a Danish fjord. ICES *J Mar Sci* 54:854-865.

Møhlenberg F, Riisgård HU (1979) Filtration rate, using a new indirect technique, in thirteen species of suspension-feeding bivalves. *Mar Biol* 54:143−148.

Okumus I, Stirling HP (1994) Physiological energetics of cultivated mussel (*Mytilus edulis*) populations in two Scottish west coast sea lochs. *Mar Biol* 119:125−131.

Riisgård HU (1998) No foundation of a "3/4 power scaling law" for respiration in biology. *Ecol Lett* 1:71−73.

Riisgård HU, Egede PP, Saavedra IB (2011a) Feeding behaviour of mussels, *Mytilus edulis*: new observations, with a mini-review of current knowledge. *J Mar Biol* (published online doi: 10.1155/2011/312459).

Riisgård HU, Jørgensen BH, Lundgreen K, Storti F, Walther JH, Meyer KE, Larsen PS (2011b) The exhalant jet of mussels *Mytilus edulis*. *Mar Ecol Prog Ser* 437:147−164.

Riisgård HU, Lundgreen K, Larsen PS (2012a) Field data and growth model for mussels *Mytilus edulis* in Danish waters. *Mar Biol Res* 8: 683-700.

Riisgård HU, Pleissner D, Lundgreen K, Larsen PS (2012b) Growth of mussels *Mytilus edulis* at algal (*Rhodomonas salina*) concentrations below and above saturation levels for reduced filtration rate. *Mar Biol Res* (in press)**.**

Riisgård HU, Randløv A, Kristensen PS (1980) Rates of water processing, oxygen consumption and efficiency of particle retention in veligers and young post-metamorphic *Mytilus edulis*. *Ophelia* 19:37−47.

Rosland R, Strand Ø, Alunno-Bruscia M, Bacher C, Strohmeir T (2009) Applying dynamic energy budget (DEB) theory to simulate growth and bio-energetics of blue mussels under low seston conditions. *J Sea Res* 62:49−61.

Saraiva S, van der Meer J, Kooijman S, Sousa T (2011) Modelling feeding processes in bivalves: A mechanistic approach. *Ecol Modell* 222:514−523.

Savage RE (1956) The great spatfall of mussels in the River Conway Estuary in Spring 1940. Fish Invest Ser II London 20:1−21.

Schütz L(1964) Die tierische Besiedlung der Hartböden in der Schweninemündung. Kieler Meeresforsch 20:198−217.

Seed R (1976) Ecology. In: Bayne BL (ed) Marine mussels: Their ecology and physiology, Cambridge University Press, Cambridge, pp 13-65.

Sprung M (1984) Physiological energetics of mussel larvae (*Mytilus edulis*). I. Shell growth and biomass. *Mar Ecol Prog Ser* 17:283−293.

Stirling HP, Okumus I (1994) Growth, mortaility and shell morphology of cultivated mussel (*Mytilus edulis*) stocks cross-planted between two Scottish sea lochs. *Mar Biol* 119:115−123.

Theisen BF (1975) Growth parameters of *Mytilus edulis* L. (Bivalvia) estimated from ragging data. Meddr fra Danm Fisk- og Havunders 7:99−109.

Thorson G (1961) Length of pelagic larval life in marine bottom invertebrates as related to larval transport by ocean currents. In: Sears M (ed) Oceanography. Washington DC, AAAS, pp 455−474.

van der Meer J (2006) Metabolic theories in ecology. *Trends Ecol Evol* 21:136−140.

van der Veer HW, Cardoso JFMF, van der Meer J (2006) The estimation of DEB parameters for various Northeast Atlantic bivalve species. *J Sea Res* 56:107−124.

Vuorinen L, Antsulevich E, Maximovich NV (2002) Spatial distribution and growth of the common mussel *Mytilus edulis* L. in the archipelago of SW-Finland, northern Baltic Sea. *Boreal Envir Res* 7:41−52.

Westerbom M, Kilpi M, Mustonen O (2002) Blue mussels, *Mytilus edulis*, at the edge of the range: population structure, growth and biomass along a salinity gradient in the north-eastern Baltic Sea. *Mar Biol* 140:991−999.

Widdows J, Donkin P, Brinsley MD, Evans SV, Salkeld PN, Franklin A, Law RJ, Waldock MJ (1995) Scope for growth and contaminant levels in North Sea mussels *Mytilus edulis*. *Mar Ecol Prog Ser* 127:131−148.